Acta Oceanol. Sin., 2019, Vol. 38, No. 4, P. 97–105
https://doi.org/10.1007/s13131-018-1337-7
http://www.hyxb.org.cn
E-mail: hyxbe@263.net

A study of intra-seasonal variations in the subsurface water temperatures in the South China Sea

Zhan Lian[1, 2], Baonan Sun[1, 2], Zexun Wei[1, 2*], Yonggang Wang[1, 2], Xinyi Wang[1]

[1] Key Laboratory of Marine Science and Numerical Modeling, First Institute of Oceanography, Ministry of Natural Resources, Qingdao 266061, China

[2] Laboratory for Regional Oceanography and Numerical Modeling, Pilot National Laboratory for Marine Science and Technology (Qingdao), Qingdao 266237, China

Received 9 February 2018; accepted 10 May 2018

Abstract

Through analysis of the results of a verified high-fidelity numerical model, the intra-seasonal variations (ISVs) in the depth of the 22°C isotherm (D22) in the South China Sea (SCS) basin are investigated. The results show that the ISVs in the D22 exhibit distinct seasonality in the SCS. The ISVs in the D22 are quite significant, especially within a band along the northwestern boundary of the basin and at the southern end of the basin during boreal winter. In these areas, the ratio of the standard deviations (STDs) of intra-seasonal band to the STDs of total data could exceed 0.6. Although the ISVs in the D22 are detectable in the area affected by the Vietnam Offshore Current during boreal summer and autumn, these variations are sometimes overwhelmed by oscillations with other frequencies. An analysis of the causes of the ISVs in the D22 in the SCS indicates that sea surface fluxes and wind stirring are not the dominant external driving mechanisms of the phenomena described above. The ISVs in the D22 are thought to be induced mainly by the thermodynamic adjustment of the ocean itself and the associated instabilities. The energy of the northern and southern bands that display strong ISVs in the D22 may be derived from eddy kinetic energy, rather than eddy available potential energy. The diversity of the propagation of the ISVs in the D22 is very conspicuous within these two bands.

Key words: intra-seasonal variations, depth of 22°C isotherm, South China Sea

Citation: Lian Zhan, Sun Baonan, Wei Zexun, Wang Yonggang, Wang Xinyi. 2019. A study of intra-seasonal variations in the subsurface water temperatures in the South China Sea. Acta Oceanologica Sinica, 38(4): 97–105, doi: 10.1007/s13131-018-1337-7

1 Introduction

The South China Sea (SCS) is one of the largest marginal seas in the West Pacific Ocean. The SCS is located in a low-latitude area, and the intra-seasonal variations (ISVs) in various oceanic features in the SCS are very significant because they are influenced by many factors, such as atmospheric forcing (Mao and Chan, 2005; Xie et al., 2007; Zhuang et al., 2010; Roxy and Tanimoto, 2011). Sengupta et al. (2001) found that the magnitude of the ISVs in sea surface temperatures (SSTs) in the SCS is highest at low latitudes. Based on satellite data and *in situ* observations, some researchers have examined other ocean surface characteristics in the SCS, such as sea surface heights (SSHs), latent heat fluxes and currents (Gao and Zhou, 2002; Wu et al., 2005; Xie et al., 2007; Zeng and Wang, 2009; Xiu et al., 2010; Zhuang et al., 2010; Chen et al., 2011) and their supplementary contributions to the atmosphere (Wu and Chen, 2015).

Firsthand observations indicate that the ISVs in the subsurface water temperatures in the SCS are substantial. These variations play a vital role in the safety of marine construction and transportation. More importantly, they can change the heat content of the ocean and impact the occurrence of the summer monsoon and precipitation in South China (Wu et al., 2007). In addition, increases in subsurface water temperatures may dramatically enhance the intensity of passing typhoons (Zheng et al., 2014). For the reasons given above, studies of the ISVs in subsurface water temperatures in the SCS are of great importance.

Based on long-term mooring data, Liu et al. (2001) and Zhou and Gao (2002) determined that this oscillation is mesoscale and that its period is less than 90 d. They also noted that the intensity of this variation is comparable to that of the annual cycle, and the mechanisms underlying this phenomenon are very complex. Nevertheless, researchers have made a certain amount of progress in the study of the ISVs in the subsurface water temperatures in the SCS; however, these results are mainly based upon sparse observations (Liu et al., 2001; Zhou and Gao, 2002; Chen et al., 2011, 2012). Given the restrictions imposed by the temporal and spatial density of the available observations, these studies do not present comprehensive descriptions of the spatiotemporal characteristics of this phenomenon. The output from numerical models, which is finely resolved, provides a more appropriate means of solving this problem. To date, few relevant studies have been published.

In this paper, we use the high-resolution Hybrid Coordinate Ocean Model and the Navy Coupled Ocean Data Assimilation

Foundation item: The National Natural Science Foundation of China under contract No. 41506037; the Basic Scientific Fund for the National Public Research Institutes of China under contract No. 2017Q06; the Natural Science Foundation of Shandong Province, China under contract No. ZR2015PD009; the NSFC-Shandong Joint Fund for Marine Science Research Centers under contract No. U1606405.

*Corresponding author, E-mail: weizx@fio.org.cn

(HYCOM + NCODA) Global (1/12)° Analysis (GLBa0.08) to investigate the ISVs in the subsurface water temperatures in the SCS. The data and methods are introduced in Section 2; the results of the model are verified in Section 3; the spatiotemporal characteristics of the ISVs in the subsurface water temperatures in the SCS are described in Section 4; an analysis of the causes of this phenomenon is presented in Section 5; and some conclusions are given in Section 6.

2 Data and methods

2.1 *Data*

To investigate the ISVs in subsurface water temperatures in the SCS, we use 13 years of output (extending from 2004 to 2016) from the HYCOM + NCODA GLBa0.08 provided by the Naval Research Laboratory of the U.S. Navy. The vertical coordinate in HYCOM remains isopycnic in the stratified open ocean but transitions smoothly to z coordinates in the weakly stratified upper-ocean mixed layer, to terrain-following sigma coordinates in shallow water regions, and back to z coordinates in very shallow water. HYCOM uses the Navy Coupled Ocean Data Assimilation (NCODA) system to assimilate data from satellite altimetry and *in situ* observations. The levels in the vertical direction are at 0, 10, 20, 30, 50, 75, 100, 125, 150, 200, 250, 300, 400, 500, 600, 700, 800, 900, 1 000, 1 100, 1 200, 1 300, 1 400, 1 500, 1 750, 2 000, 2 500, 3 000, 3 500, 4 000, 4 500, 5 000, and 5 000 m. The surface forcing is derived from the Navy Operational Global Atmosphere Prediction System (NOGAPS) and the Navy Global Environmental Model (NAVGEM).

To verify the reliability of the model results, we compare several *in situ* observational temperature profiles with the simulation. The observations are derived from the World Ocean Database (WOD), Argo data, the Global Temperature-Salinity Profile Programme (GTSPP), the open cruises of the National Natural Science Foundation of China (NSFC), and the cruises of the National Basic Research Program of China and the Response of Marine Hazards to Climate Change in the Western Pacific Project (ROSE) conducted by the First Institute of Oceanography, State Oceanic Administration, People's Republic of China.

Note that long-term *in situ* observations may be most appropriate in examining the ISVs in subsurface temperature produced by the simulation. However, few such highly appropriate data collected at moorings with onboard temperature-salinity-depth sensor chains are available. Therefore, many momentary temperature profiles are used to evaluate the statistical and systematic differences in the transient vertical temperature distribution between the simulation and the observations.

2.2 *Methods*

As indicated by Liu et al. (2001), the variations in the 22°C isotherm in the SCS are closely related to those of the thermocline; therefore, we take the depth of the 22°C isotherm (D22) as an index of subsurface water temperatures in the SCS.

To extract the intra-seasonal variability, we use a 10- to 90-d bandpass filter, as is common in studies of ISVs. We calculate the standard deviation (STD) of the filtered data to indicate the intensity of the ISVs.

The processes that produce vertical mixing in shallow seas are complex, and many dynamic and thermal factors may affect the subsurface water temperatures. It is more challenging to reproduce the vertical temperature profile in the shallow seas than that in the open ocean basin in a numerical model. Thus, to improve the accuracy of this study, we consider only the parts of the SCS with water depths exceeding 200 m.

3 Verification

The locations of all of the observed temperature profiles are presented in Fig. 1a. As shown in the figure, these profiles are abundant in the SCS basin, thanks to the long-term accumulation of data from multiple sources. Measured profiles are especially abundant in the northern part of the SCS. However, the density of temperature profiles is still relatively sparse in the southern part of the SCS basin. Only certain cruises, such as those of the ROSE project, have collected CTD observations in this area.

Figure 1b compares the observed and simulated D22 values. In this figure, the x-axis indicates the model results, whereas the y-axis indicates the corresponding observations. The correlation

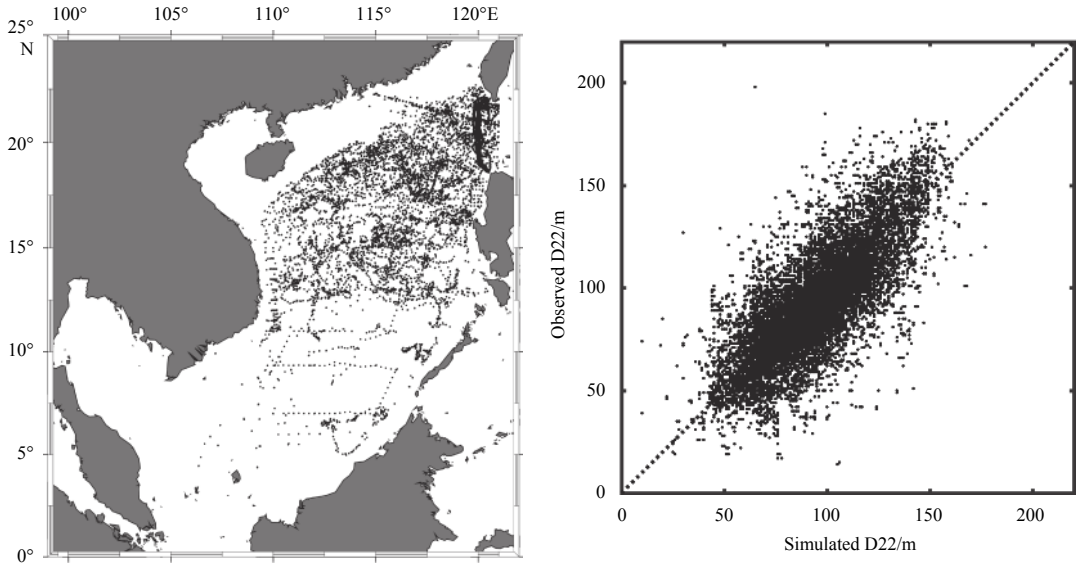

Fig. 1. The locations of all observational temperature profiles (a) and a scatter diagram of the simulated D22 (x-axis) versus the observed D22 (y-axis) (b).

coefficient between the simulation results and the observations is 0.73. The absolute deviation and annual mean of the simulated D22 values are 11.2 m and 92.0 m, whereas the absolute deviation and annual mean of the observed D22 values are 15.6 m and 91.5 m. In general, the points are distributed along the diagonal line of the coordinate system. This result implies that, from a statistical perspective, the simulation yields highly reliable transient D22 values in the SCS. This verification provides a basis for the following analysis of the ISVs in the D22 in the SCS.

4 The ISVs in the D22 in the SCS

We apply a high-pass filter to the model results and calculate the STD of the 13 years of data. The climatological and annual mean STDs of the ISVs in the D22 are presented in Fig. 2. In Figs 2a–e, the colors indicate the STDs of the ISVs in the D22, whereas the black contours represent the climatological mean D22.

These figures indicate that the ISVs in the D22 are most prominent during boreal winter in the SCS. During this time, the most active ISVs in the D22 emerge along the northwestern boundary of the SCS basin and extend westward from the Luzon Strait. The maximum intensity in this region exceeds 20 m. Another region of active ISVs in the D22 is located at the southern end of the SCS basin; the area and the magnitude of the ISVs in the south region are less than those of the northwestern boundary of the SCS basin. In addition, the average intensity of the ISVs in the D22 in the entire basin exceeds 10 m. The results for the spring represent a transition state. The spatial pattern is similar to that during winter, except that the southern region of active ISVs disappears, and the magnitudes are smaller. The spatial distribution of the ISVs in the D22 in the SCS during summer and autumn differs notably from that during winter and spring. In summer and autumn, the active ISVs in the D22 extend from southwest to northeast across the SCS basin. The intensity is relatively low in the southeastern part of the SCS basin. The belt of high ISV activity along the northwestern boundary of the basin almost disappears, and only some parts of this belt persist in the west of the Luzon Strait. This seasonal variation coincides with the incursion of the Kuroshio Current. To the south of this area, offshore from the east coast of the Indo-China Peninsula, a core of high ISV activity appears that differs notably from that during winter and spring. This phenomenon is more significant in autumn, and it may be correlated with another circulation system, the Vietnam Offshore Current (VOC). Conversely, in the eastern part of the SCS basin, the ISVs in subsurface temperatures reflect relatively small changes during summer and autumn.

It is worthwhile to compare the intensities of the ISVs in the D22 with those of oscillations that operate at other time scale, for example, the seasonal, annual and decadal oscillations. The ratios of the STDs of intra-seasonal band to the STDs of total data are shown in Fig. 2f. In this figure, the colors indicate the ratios, and the 0.6 isoline is shown as a solid black line. Consistent with the climatological results for winter and autumn, the ISVs in subsurface temperatures are larger along the northwestern boundary of the SCS basin and at its southern end. In these areas, the ISV ratio could exceed 0.6. However, although there is a zone of high ISV activity offshore of the east coast of the Indo-China Peninsula in summer and autumn, the STDs associated with the ISVs are overwhelmed by the other oscillations.

This analysis shows that the temporal and spatial features of the ISVs in the D22 in the SCS are similar to those of the ocean surface factors to some degree. For instance, both the ISVs in the D22 and the ISVs in SSHs display obvious seasonal differences (Zhuang et al., 2010). In addition, the ISVs in the D22 show parallels with the ISVs in the SSTs in the area affected by the VOC (Xie et al., 2007). However, there is a non-negligible divergence between the ISVs in the D22 and the ISVs in the surface factors. For example, there is a striking core of high ISVs in the D22 at the

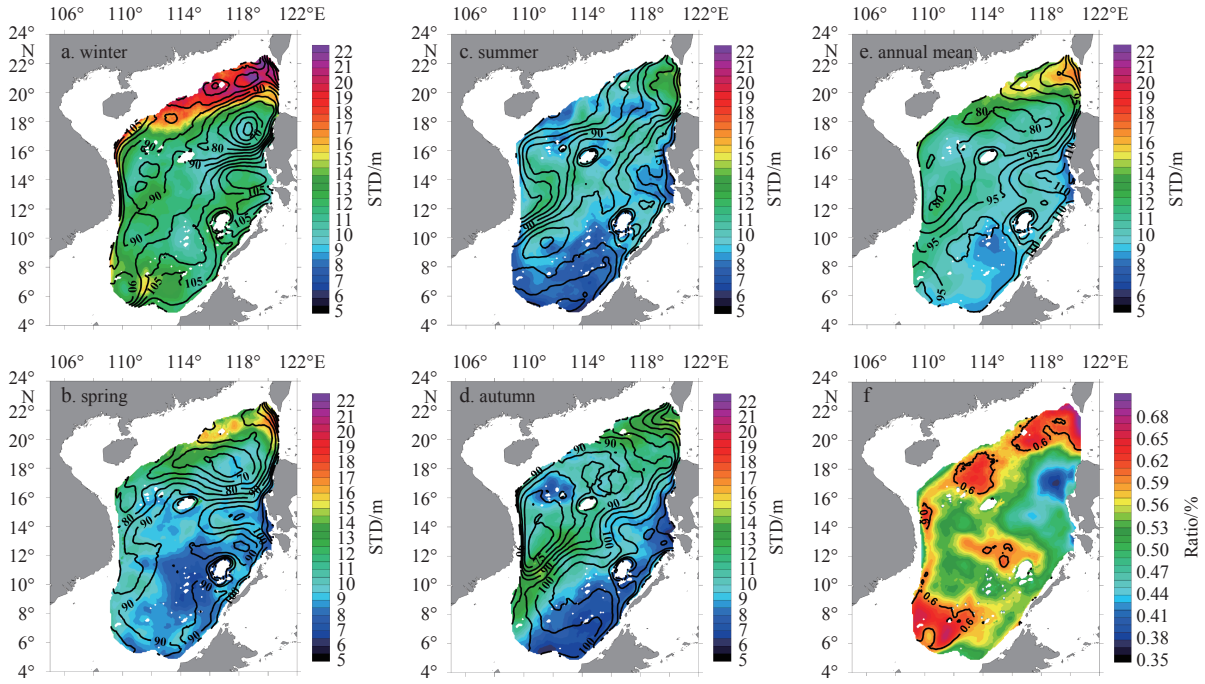

Fig. 2. The spatial distribution of the STDs associated with the ISVs in the D22 (shaded areas) of SCS for winter (a), spring (b), summer (c), autumn (d), the annual mean (e), and the ratio of the STDs of intra-seasonal band to the STDs of total data (f). The climatological D22 is shown as black contours in a–e.

southern end of the SCS in winter, and the relative magnitude of the ISVs in the D22 along the coast of Vietnam is less prominent in summer and autumn. These results suggest that the mechanism that produces the ISVs in the D22 may not be the same as those that produce the ISVs in the SSTs and SSHs.

5 An analysis of the causes of the intra-seasonal variations in the D22 in the SCS

Both dynamic and thermal processes may generate the ISVs in the D22; wind stirring and heating are two of the main external forcings that drive these processes. To investigate the contributions from these external forcings to the ISVs in the D22, we calculate the pointwise correlation coefficients between the intra-seasonal D22 and the net heat flux at the sea surface (Fig. 3) and the sea surface wind curl (Fig. 4). The positive net heat flux refers to the heat transport from atmosphere to ocean.

According to the principles that govern thermal processes, increases in the heat flux should be accompanied by increases in the D22. However, the results indicate the opposite behavior. In winter, the analysis essentially reflects a negative correlation between the intra-seasonal D22 and the variations in the sea surface heat flux over the entire SCS basin. The reason might be that the enhancing of the upper ocean heat content that accompanies an increase in the D22 would make the ocean heat the overlying atmosphere, thus reducing the surface heat flux. The negative correlation is more significant in winter and in the northwestern portion of the SCS basin in summer and autumn because the D22 is shallower in those areas. It might be argued that external heating is not the main driver of the ISVs in the D22 in the SCS basin.

Although classical dynamical theory suggests that positive wind curl may reduce the D22, a robust negative correlation between the intra-seasonal D22 and the sea surface wind curl is not seen in the results, except that this correlation is only just distinguishable within the area affected by the VOC in summer. This result implies that the wind stirring indeed strengthens the ISVs in the D22 in the SCS; however, this conclusion is only partially correct, and the strength of this effect depends on time and

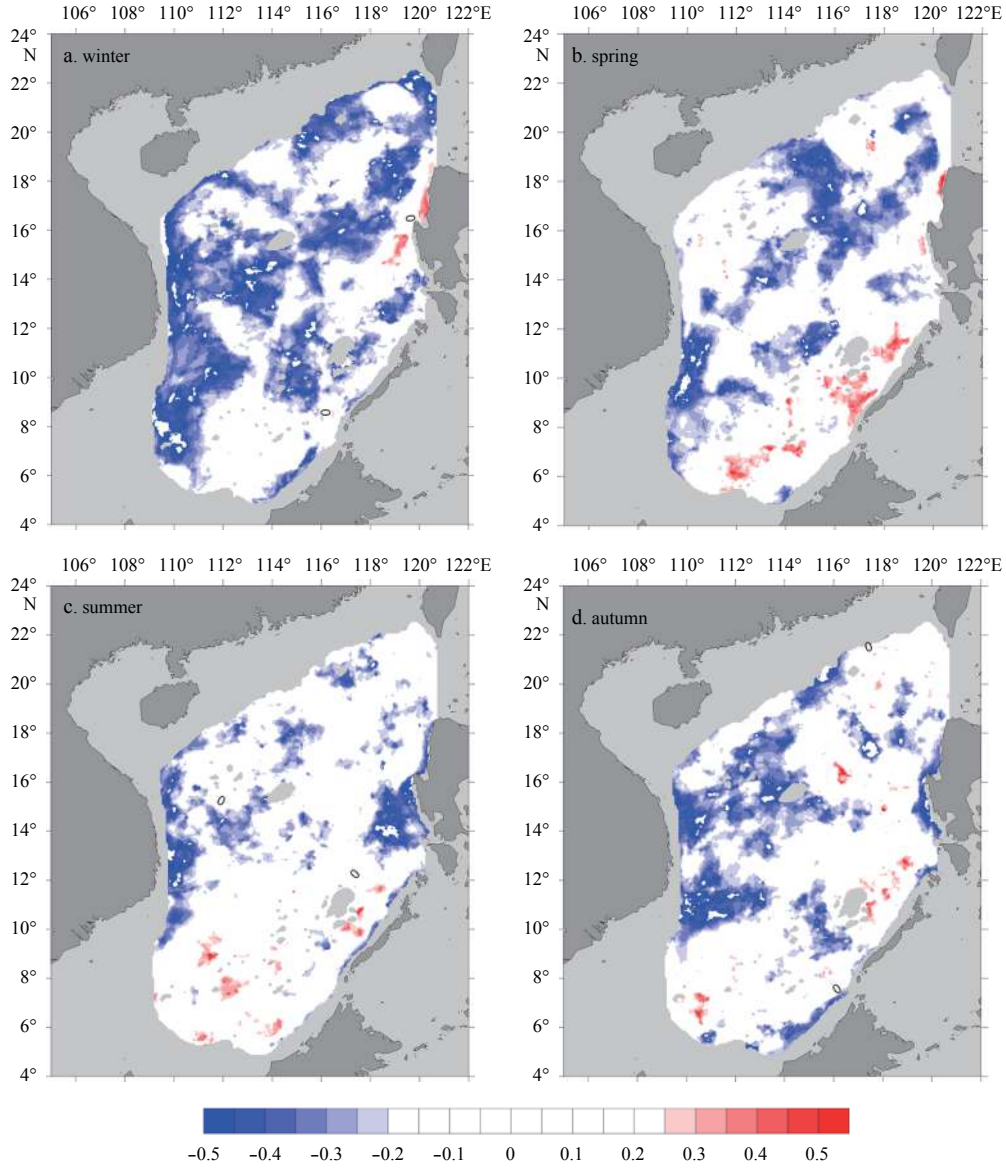

Fig. 3. Pointwise correlation coefficients between the ISVs in the D22 and the sea surface heat flux in winter (a), spring (b), summer (c), and autumn (d). The shaded zone is over 95% confidence levels.

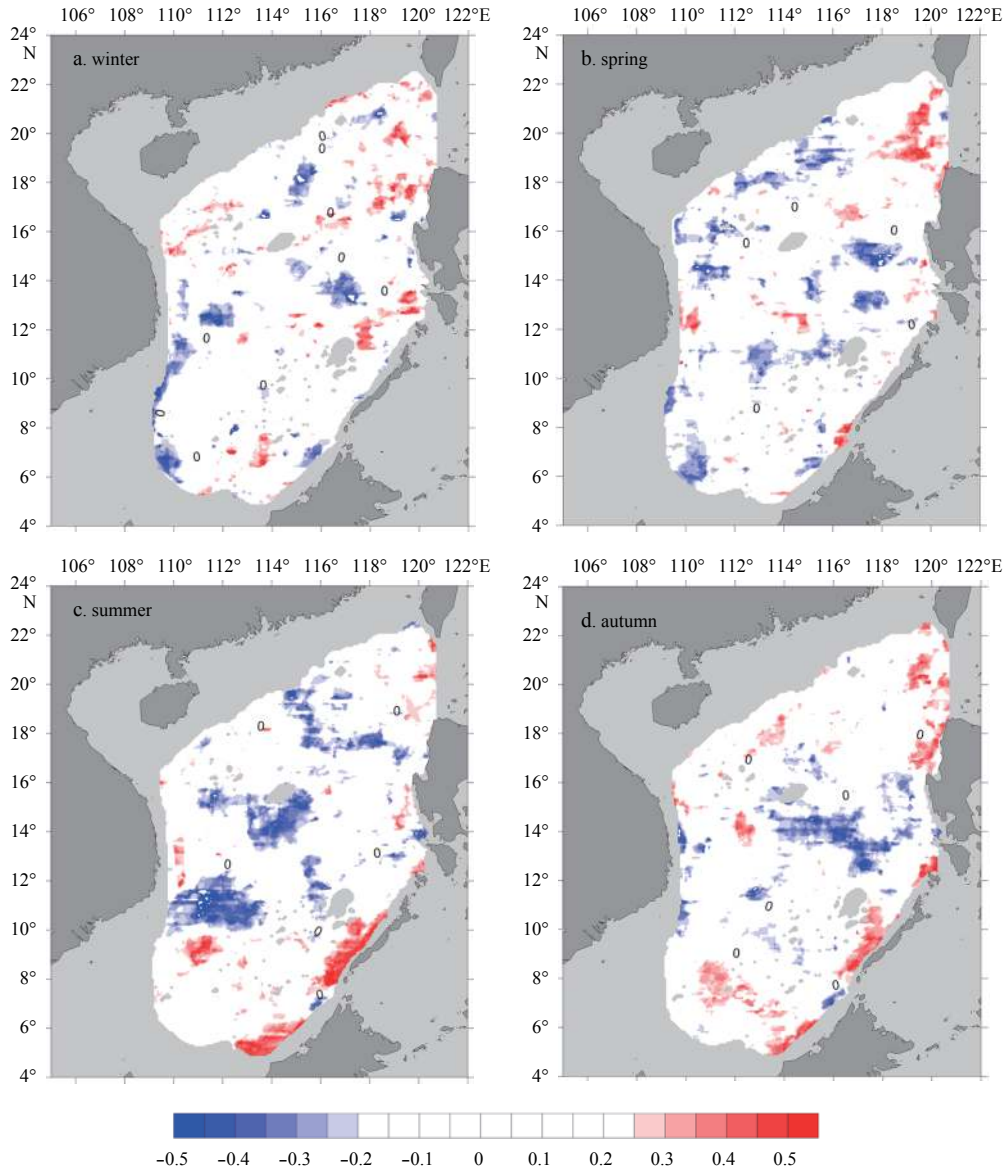

Fig. 4. Pointwise correlation coefficients between the ISVs in the D22 and the sea surface wind curl in winter (a), spring (b), summer (c), and autumn (d). The shaded zone is over 95% confidence levels.

space.

We also calculate the correlation coefficients between the ISVs in the D22 and the buoyancy flux, but the correlation is not especially distinct (the results are not shown here).

The above analysis suggests that external forcings are not the dominant driver of the ISVs in the D22 in the SCS. Instead, this phenomenon likely arises due to internal adjustments of the ocean itself. To identify the energy sources of this adjustment, the eddy kinetic energy (EKE) and the eddy available potential energy (EPE) are calculated. These quantities are defined as follows:

$$\mathrm{EKE} = \frac{1}{2}\left(u'^2 + v'^2\right),$$

$$\mathrm{EPE} = -\frac{g\tilde{\rho}'^2}{2\rho\left(\partial\bar{\rho}_\theta/\partial z\right)},$$

where $\tilde{\rho}\left(x,y,z,t\right) = \rho\left(x,y,z,t\right) - \rho_\mathrm{b}\left(z\right)$, $\rho_\mathrm{b}(z)$ is the background density profile, which is calculated as the annual and horizontal mean within the SCS, and $\bar{\rho}_\theta$ is the annual and horizontal mean potential density. The transient components of the velocity and density are defined as the variability over periods ranging from 10 to 90 d, and the residual low-frequency variations are treated as the base state. The climatological EKE and EPE are illustrated in Figs 5 and 6, respectively.

According to the results, some cores of high ISVs in the D22 occur in the same places as the areas with high EKE. Examples include the band along the northwestern boundary and the southern end of the basin in winter. However, the EPE is not especially high in these two areas. This result indicates that, at these specific locations and at particular times, the thermodynamic adjustment of the ocean associated with the ISVs in the D22 is driven mainly by EKE, rather than EPE. During summer and autumn, in the area offshore of the coast of Vietnam, the EPE and EKE are both strikingly high. This co-occurrence of high EPE and EKE values would induce a vigorous energy cascade, which

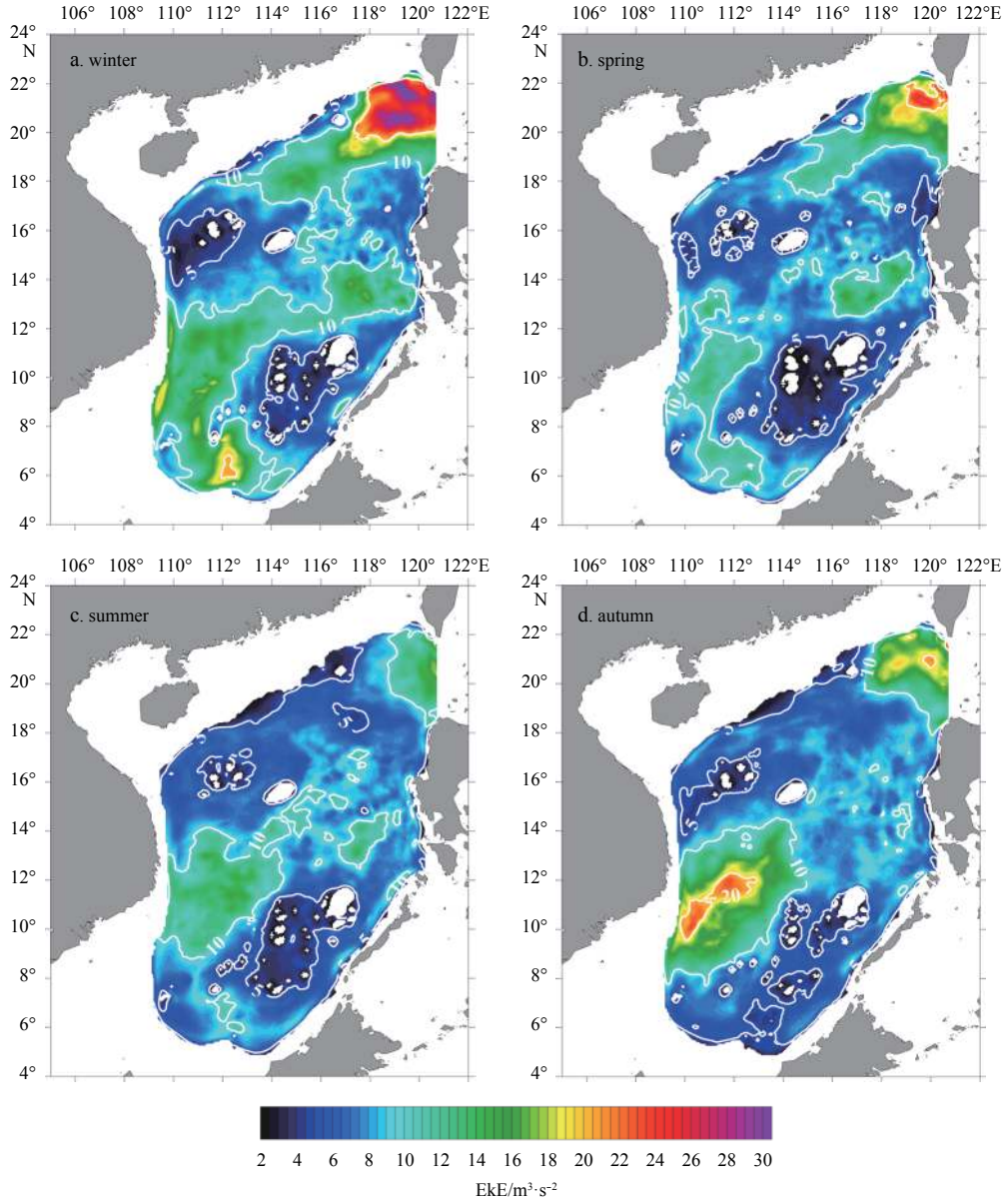

Fig. 5. The vertical integrated EKE in the SCS basin for winter (a), spring (b), summer (c), and autumn (d).

may partly explain why the ISVs are attenuated by variations on other time scales, as demonstrated in Fig. 2f. Although EPE is abundant in the southeastern portion of the SCS basin during summer and autumn, the ISVs in the D22 are in a period of inactivity. This implies that energy conversion plays a vital role in the genesis of the ISVs in the D22, and investigations of barotropic and baroclinic instability are needed.

To investigate the propagation of the ISVs in the D22 in the SCS basin, Fig. 7 shows the lag correlation of the ISVs in the D22 along the band of high variability that extends from west of the Luzon Strait towards the western boundary of the basin (Line A in Fig. 7a) and is nearly parallel with the Vietnamese coast (Line B in Fig. 7a). The D22 values at the midpoint of this line are taken as the reference time series. Along Line A, the ISVs display a pronounced southwestward propagation during the December–March (DJFM) active season but are somewhat localized during the July–September (JJAS) inactive season. During DJFM, the typical oscillation period is 50–60 d. The typical phase speed varies; it is approximately 10 cm/s in the northern section, whereas it is approximately 5 cm/s in the southern section. Thus, the propagation of D22 variability along Line A may be forced or affected by different factors. The propagation might be influenced by eddies, the mean flow and Rossby waves. The correlation is weak in the Luzon Strait, indicating that intra-seasonal perturbations do not generally propagate directly from the West Pacific. Instead, the ISVs in the D22 in the northern band are generated locally just west of the Luzon Strait and then propagate southwestward, consistent with previous analyses (Li et al., 2007; Wu and Chiang, 2007).

In contrast, the ISVs in the D22 do not display robust propagation patterns during either the DJFM inactive period or the JJAS active period. It is consistent with the result that the D22 ISV along VOC is high correlated with the local wind stress curl in summer. Basically, the high correlation is unevenly located in the lag 0 band, indicating that the ISVs emerge systematically and synchronously along the southern and northern parts of the line

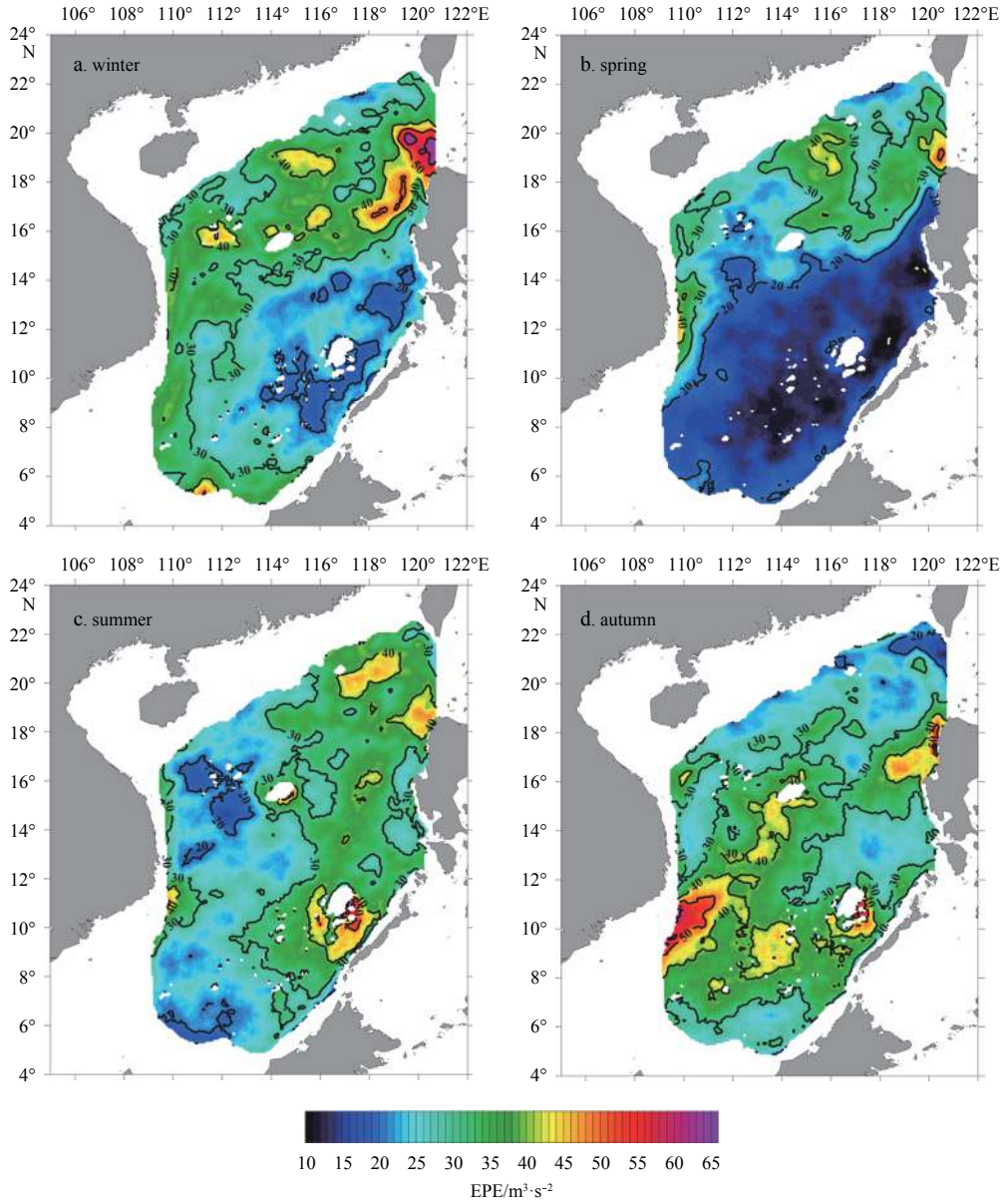

Fig. 6. The vertical integrated EPE in the SCS basin for winter (a), spring (b), summer (c), and autumn (d).

during DJFM and JJAS, respectively.

6 Conclusions

Through an analysis of the output from a verified high-fidelity numerical model, the ISVs in the D22 in the SCS basin are investigated. The results show that the ISVs in the D22 in the SCS display distinct seasonality. The ISVs in the D22 are quite significant during boreal winter, especially in the band along the northwestern margin of the basin and at the southern end of the basin. In these areas, the ratio of the STDs of intra-seasonal band to the STDs of total data could exceed 0.6. The ISVs in the D22 display substantial activity in the area affected by the VOC in summer and autumn; however, this variation is sometimes overwhelmed by oscillations at other frequencies.

An analysis of the causes of the ISVs in the D22 in the SCS indicates that the sea surface flux and wind stirring are not the dominant external driving mechanisms of the phenomena described above. The ISVs in the D22 are sometimes even negatively correlated with the sea surface heat flux. The ISVs in the D22 are inferred to be induced mainly by the thermodynamic adjustment of the ocean itself and the associated instability. The energy of the northern and southern zones that display high ISVs in the D22 may be associated with EKE, rather than EPE. In contrast, both EKE and EPE are abundant offshore of the coast of Vietnam. The co-occurrence of high levels of both EKE and EPE enhances not only the ISVs but also the variations at other frequencies.

The diversity of the propagation of the ISVs is very conspicuous in the southern and northern regions with notably high ISVs in the D22. Within the northern band, the propagation is more obvious during DJFM. In addition, it is challenging to identify propagation of the ISVs in the D22 at other places and times. These results further confirm that the mechanism that produces the ISVs in the D22 varies temporally and spatially within the SCS basin.

As indicated above, the correlation analysis shows that the

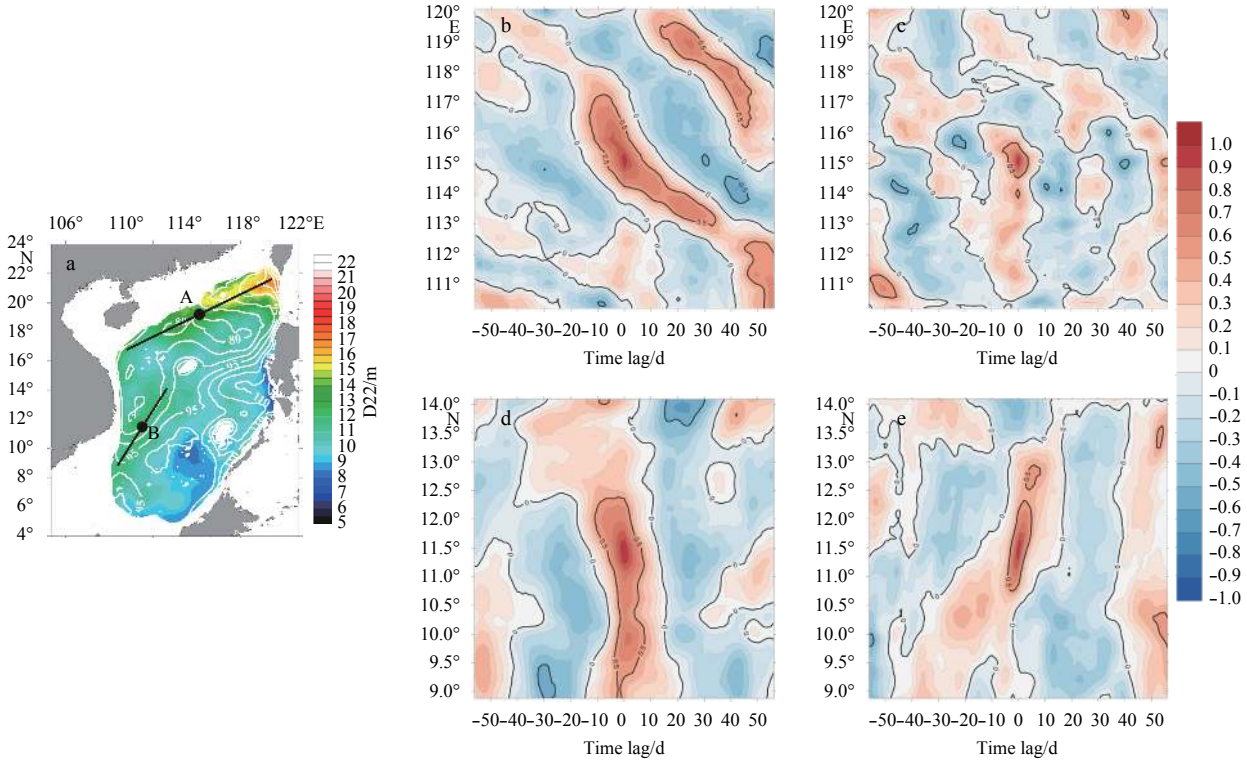

Fig. 7. Spatiotemporal lag correlation of the ISVs in the D22 along Lines A and B (indicated by solid black lines in a; the colors represent the annual mean D22) during December–March (Line A) (b), and during June–September (Line A) (c); and d and e are the same as b and c, but for Line B.

ISVs in the D22 do not result directly from atmospheric forcing; thus, it might be less likely to identify a relationship between the ISVs in the D22 and atmospheric phenomena, such as the Madden-Julian Oscillation, except off the eastern coast of Vietnam, where the sea surface wind curl displays a comparatively close relationship with the ISVs in the D22.

It is noteworthy that the locations of zones that display active ISVs in the D22 do not coincide perfectly with the areas of high energy. Energy conversion and the propagation of the ISVs in subsurface water temperatures represent potential reasons for this characteristic. Intensive investigations are crucial in understanding the genesis and underlying mechanisms of the ISVs in subsurface water temperatures.

Acknowledgements

Funding for the development of HYCOM was provided by the National Ocean Partnership Program and the Office of Naval Research. The production of data assimilation products using HYCOM is funded by the U.S. Navy. Computer time is made available by the DoD High Performance Computing Modernization Program. The output is publicly available at http://hycom.org. We thank Qiang Xie and Hongzhou Xu for their help in downloading and exchanging the data. The observational temperature profiles were provided by the National Marine Data & Information Service, China. We also thank all personnel who perform the marine observation and data service.

References

Chen Gengxin, Gan Jianping, Xie Qiang, et al. 2012. Eddy heat and salt transports in the South China Sea and their seasonal modulations. Journal of Geophysical Research: Oceans, 117(C5): C05021

Chen Gengxin, Hou Yijun, Chu Xiaoqing. 2011. Mesoscale eddies in the South China Sea: mean properties, spatiotemporal variability, and impact on thermohaline structure. Journal of Geophysical Research: Oceans, 116(C6): C06018

Gao Rongzhen, Zhou Faxiu. 2002. Monsoonal characteristics revealed by intraseasonal variability of Sea Surface Temperature (SST) in the South China Sea (SCS). Geophysical Research Letters, 29(8): 1222

Li Li, Jing Chunsheng, Zhu Dayong. 2007. Coupling and propagating of mesoscale sea level variability between the western Pacific and the South China Sea. Chinese Science Bulletin, 52(12): 1699–1707, doi: 10.1007/s11434-007-0203-3

Liu Qinyu, Jia Yinglai, Liu Penghui, et al. 2001. Seasonal and intraseasonal thermocline variability in the central south China Sea. Geophysical Research Letters, 28(13): 4467–4470

Mao Jiang, Chan J C L. 2005. Intraseasonal variability of the South China Sea summer monsoon. Journal of Climate, 18(13): 2388–2402, doi: 10.1175/JCLI3395.1

Roxy M, Tanimoto Y. 2011. Influence of sea surface temperature on the intraseasonal variability of the South China Sea summer monsoon. Climate Dynamics, 39(5): 1209–1218

Sengupta D, Goswami B N, Senan R. 2001. Coherent intraseasonal oscillations of ocean and atmosphere during the Asian Summer Monsoon. Geophysical Research Letters, 28(21): 4127–4130, doi: 10.1029/2001GL013587

Wu C R, Chiang T L. 2007. Mesoscale eddies in the Northern South China Sea. Deep Sea Research Part II: Topical Studies in Oceanography, 54(14–15): 1575–1588, doi: 10.1016/j.dsr2.2007.05.008

Wu C R, Tang T Y, Lin S F. 2005. Intra-seasonal variation in the velocity field of the northeastern South China Sea. Continental Shelf Research, 25(17): 2075–2083, doi: 10.1016/j.csr.2005.03.005

Wu Disheng, Wei Jiansu, Zhou Shuihua, et al. 2007. Subsurface sea

temperature in north and middle South China Sea, monsoon, drought and flood in Guangdong. Journal of Tropical Meteorology (in Chinese), 23(6): 581–586

Wu Renguang, Chen Zhang. 2015. Intraseasonal SST variations in the South China Sea during boreal winter and impacts of the East Asian winter monsoon. Journal of Geophysical Research: Atmospheres, 120(12): 5863–5878, doi: 10.1002/2015JD023368

Xie Shangping, Chang C H, Xie Qiang, et al. 2007. Intraseasonal variability in the summer South China Sea: wind jet, cold filament, and recirculations. Journal of Geophysical Research, 112(C10): C10008, doi: 10.1029/2007JC004238

Xiu Peng, Chai Fei, Shi Lei, et al. 2010. A census of eddy activities in the South China Sea during 1993-2007. Journal of Geophysical Research: Oceans, 115(C3): C03012

Zeng Lili, Wang Dongxiao. 2009. Intraseasonal variability of latent-heat flux in the South China Sea. Theoretical and Applied Climatology, 97(1–2): 53–64, doi: 10.1007/s00704-009-0131-z

Zheng Yan, Cai Qinbo, Cheng Shouchang, et al. 2014. Characteristics on intensity and precipitation of super typhoon Rammasun (1409) and reason why it rapidly intensified offshore. Torrential Rain and Disasters (in Chinese), 33(4): 333–341

Zhou Faxiu, Gao Rongzhen. 2002. Intraseasonal variability of the subsurface temperature observed in the South China Sea (SCS). Chinese Science Bulletin, 47(4): 337–342, doi: 10.1360/02tb9081

Zhuang Wei, Xie Shangping, Wang Dongxiao, et al. 2010. Intraseasonal variability in sea surface height over the South China Sea. Journal of Geophysical Research: Oceans, 115(C4): C04010